THE JOURNAL OF PHYSICAL CHEMISTRY B

Article

pubs.acs.org/JPCB

Fragmentation Processes of Hydrogen-Deficient Peptide Radicals in Matrix-Assisted Laser Desorption/Ionization In-Source Decay Mass Spectrometry

Daiki Asakawa[†,‡] and Mitsuo Takayama*[,†]

[†]Graduate School in Nanobioscience, Mass Spectrometry Laboratory, Yokohama City University, 22-2 Seto, Kanazawa-ku, Yokohama, Japan

[‡]Department of Chemistry, Mass Spectrometry Laboratory, University of Liege, Liege 4000, Belgium

ABSTRACT: The mechanism of in-source decay (ISD) in matrix-assisted laser desorption/ionization (MALDI) has been described. The MALDI-ISD with an oxidizing matrix is initiated by hydrogen abstraction from peptides to matrix molecules, leading to hydrogen-deficient peptide radicals. Subsequently, the C_α–C and C_α–H bonds are cleaved, forming the $a\bullet/x$ fragment pair and [M−2H], respectively. Those reactions competitively occur during MALDI-ISD processes. Our results suggest that the C_α–H bond cleavage to form [M−2H] was induced by collisions between hydrogen-deficient peptide radicals and matrix molecules in the MALDI plume. In contrast, the C_α–C bond cleavages occur via a unimolecular dissociation process and independently of the collision rate in the MALDI plume. The formation mechanism of the *a*-, *b*-, and *d*-series fragments are also described. We report 2,5-bis(2-hydroxyethoxy)-7,7,8,8-tetracyanoquinodimethane (bisHE-TCNQ), being known as an organic semiconductor and an electron acceptor, as a novel suitable matrix for the MALDI-ISD of peptides via hydrogen abstraction.

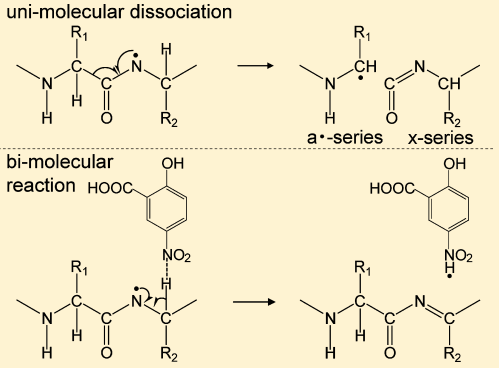

INTRODUCTION

Mass spectrometry has been used as a powerful analytical tool in a wide variety of scientific fields because of its high sensitivity and rapidity. Of the soft ionization methods, matrix-assisted laser desorption/ionization (MALDI)[1−3] and electrospray ionization (ESI)[4,5] are recognized as indispensable analytical methods for identifying peptides and proteins. In particular, peptide-mass fingerprinting (PMF) with MALDI-MS has become a common approach for the characterization of proteins.[6,7] PMF is essential for the identification process that desorption/ionization occur without fragmentation.

MALDI often can lead to fragmentation during the desorption/ionization process. This fragmentation is observed either as in-source decay (ISD)[8] or postsource decay (PSD).[9,10] Both ISD and PSD have been used for the amino acid sequencing of peptides.[11,12] ISD is a fragmentation occurring in the MALDI source, rapidly after the laser shot and before the ion extraction, while PSD is a fragmentation of metastable ions occurring in the field-free drift path of the time-of-flight mass spectrometer. PSD fragment ions can be revealed by a reflectron time-of-flight mass spectrometer. The mechanisms of ISD and PSD are extremely different. In PSD, the observable *a*-, *b*-, and *y*-series ions can be explained by vibration activation processes.[12] During the desorption/ionization process, the excess energy deposited on the peptide ions is converted into vibrational energy that is distributed over the molecule, leading to fragmentations. Therefore, the larger peptides and even proteins decreased the fragmentation efficiency due to the less energy received per degree of freedom.

In contrast to PSD, ISD has been utilized as a tool for amino acid sequencing of proteins,[13−15] because of the strong propensity for N–C_α bond cleavage to occur without degradation of side-chains. ISD is initiated by the hydrogen transfer from excited matrix molecules to the carbonyl oxygen of peptide backbone, leading to a hypervalent peptide.[16] Subsequently, the N–C_α bond on the peptide backbone is cleaved, leading to the formation of the $c'/z\bullet$ fragment pair.[17] The $z\bullet$-series ions undergo either loss of a hydrogen atom or gain of a hydrogen atom or react with a matrix radical after the N–C_α bond cleavage.[17]

Recently, we found that 5-nitrosalicylic acid (5-NSA) as a matrix for MALDI-ISD resulted in the generation of *a*- and *x*-series ions accompanied with oxidized peptide ion $[M-2H+H]^+$.[18,19] The MALDI-ISD with 5-NSA is initiated by hydrogen transfer from the amide nitrogen of the peptide backbone to the matrix molecule.[18] The hydrogen abstraction from peptides results in the formation of hydrogen-deficient peptide radicals [M−H]• containing a radical site on the amide nitrogen with subsequent radical-induced cleavage at the C_α–C bonds, leading to the $a\bullet/x$ fragment pair.[19] The $a\bullet$-series ions undergo further hydrogen abstraction to form the *a*-series ions

Received: November 8, 2011
Revised: February 28, 2012
Published: February 28, 2012

after C_α–C bond cleavage (Scheme 1).[19] Since the Pro residue cannot have a nitrogen-centered radical site, C_α–C bond

Scheme 1. C_α–C Bond Cleavage via Hydrogen Abstraction

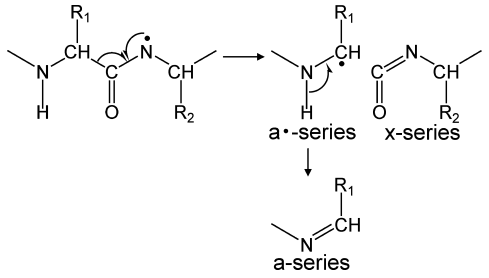

cleavage does not occur. Alternatively, the specific cleavage of CO–N bond cleavage at Xxx–Pro was observed *via* hydrogen abstraction from the C_α–H in the Pro residue.[19] The CO–N bond cleavage leads to the formation of the *b*•/*y* fragment pair, and the *b*•-series ions undergo further degradation to form the *b*- and *a*-series ions after the CO–N bond cleavage (Scheme 2).[19] The use of 5-NSA provides useful complementary

Scheme 2. CO–N Bond Cleavage at Xxx–Pro via hydrogen Abstraction

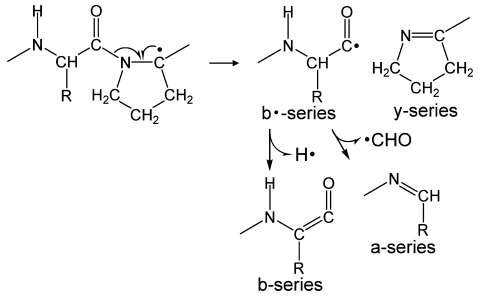

information to the MALDI-ISD with reducing matrix for the analysis of amino acid sequencing and site localization of phosphorylation in peptides.[20]

The 7,7,8,8-tetracyanoquinodimethane (TCNQ), being known as an electron acceptor in intermolecular charge-transfer materials, has been reported to be a particularly suitable positive-ion MALDI matrix for polycyclic aromatic hydrocarbons and industrial pigments.[21−23] In contrast, tetrathiafulvalene (TTF), an electron donor in intermolecular charge-transfer materials, can be used as a matrix for industrial pigments in negative-ion MALDI-MS.[24]

In this study, we report TCNQ derivative as a new oxidizing matrix for the MALDI-ISD of peptide. The influence of the initial velocity of analyte ions on the yield of ISD fragment ions is also described.

EXPERIMENTAL SECTION

Materials. The peptides, ACTH 18-35 and bradykinin potentiator B, were purchased from Peptide Institute (Osaka, Japan), and [Sar^9, Met(O$_2$)^{11}]-substance P was purchased from Sigma-Aldrich (St. Louis, MO, USA). The sequences of peptides used are summarized in Table 1. TCNQ was purchased from Sigma-Aldrich (St. Louis, MO, USA). 2,5-Bis(2-hydroxyethoxy)-7,7,8,8-tetracyanoquinodimethane (bisHE-TCNQ) and 5-NSA were purchased from Tokyo Kasei (Tokyo, Japan). Their molecular structures are shown in

Table 1. Monoisotopic Mass (M_m) and Sequence of Analyte Peptides Used

analyte peptide	M_m	sequence
ACTH18-35	1978.0	RPVKVYPNGAEDESAEAF
[Sar^9, Met(O$_2$)^{11}]-substance P	1392.7	RPKPQQFFSarLM(O$_2$)-NH$_2$
bradykinin potentiator B	1181.7	Pyr-GLPPRPKIPP

Scheme 3. Trifluoroacetic acid and acetonitrile were purchased from Wako Pure Chemicals (Osaka, Japan). All reagents were

Scheme 3. Structures of the Matrixes Investigated: TCNQ, bisHE-TCNQ, and 5-NSA

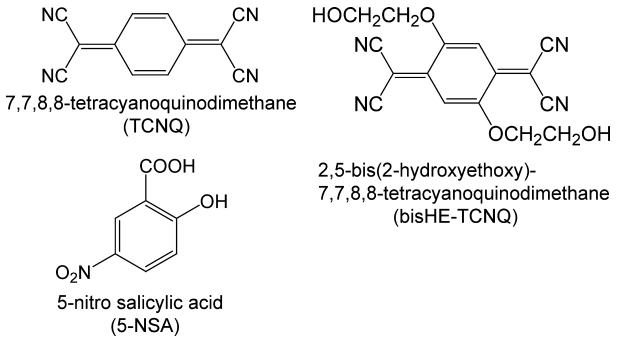

used without further purification except for water, which was purified through a Milli-Q water purification system (Millipore; Billerica, MA, USA).

Sample Preparation. Analyte peptides were dissolved in water at a concentration of 20 pmol/μL. 5-NSA (10 mg/mL) and bisHE-TCNQ (saturated solution) were dissolved in water/acetonitrile (1:1, v/v) with 0.1% TFA. A 5 μL portion of analyte solution was mixed with 5 μL of matrix solution. A volume of 1 μL of sample solution was deposited onto a stainless steel plate, and the solvents were removed by allowing evaporation in air at room temperature. TCNQ was dissolved in acetone at a concentration of 10 mg/mL. A volume of 0.5 μL of analyte solution was deposited onto a stainless-steel MALDI target and left to dry. After complete evaporation of the solvent, 0.5 μL of TCNQ solution in acetone was deposited onto the dried peptides.

Matrix-Assisted Laser Desorption/Ionization Mass Spectrometry. MALDI-ISD mass spectra were recorded using an AXIMA-CFR time-of-flight (TOF) mass spectrometer (Shimadzu, Kyoto, Japan) equipped with a nitrogen laser (337 nm wavelength, 4 ns pulse width, 10 Hz pulse rate). Ions generated by MALDI were accelerated through a 20 kV potential with delayed extraction. For the MALDI-ISD analysis, the analyzer operated in the reflectron mode. A total of 500 shots were accumulated for each mass spectrum.

For the measurement of the axial initial velocity of analytes, the analyzer operated in the linear mode. A total of 500 shots were accumulated for each mass spectrum acquisition. The arrival times were evaluated by averaging 5 times measurement.

Notation. We employed herein the unambiguous notation of Zubarev when naming the fragment ions.[25] According to this notation, homolytic C_α–C bond cleavage yields the radical fragments *a*• and *x*•, and loss of a hydrogen atom from an *a*• or *x*• fragment produces an *a* or *x* fragment, respectively. The product of a hydrogen atom transfer to an *a*• or *x*• fragment is denoted *a*′ and *x*′, respectively. Thus, *a* and *x* fragments are 1.0078 Da smaller than *a*• and *x*• fragments, respectively, and

dx.doi.org/10.1021/jp210728s | J. Phys. Chem. B 2012, 116, 4016−4023

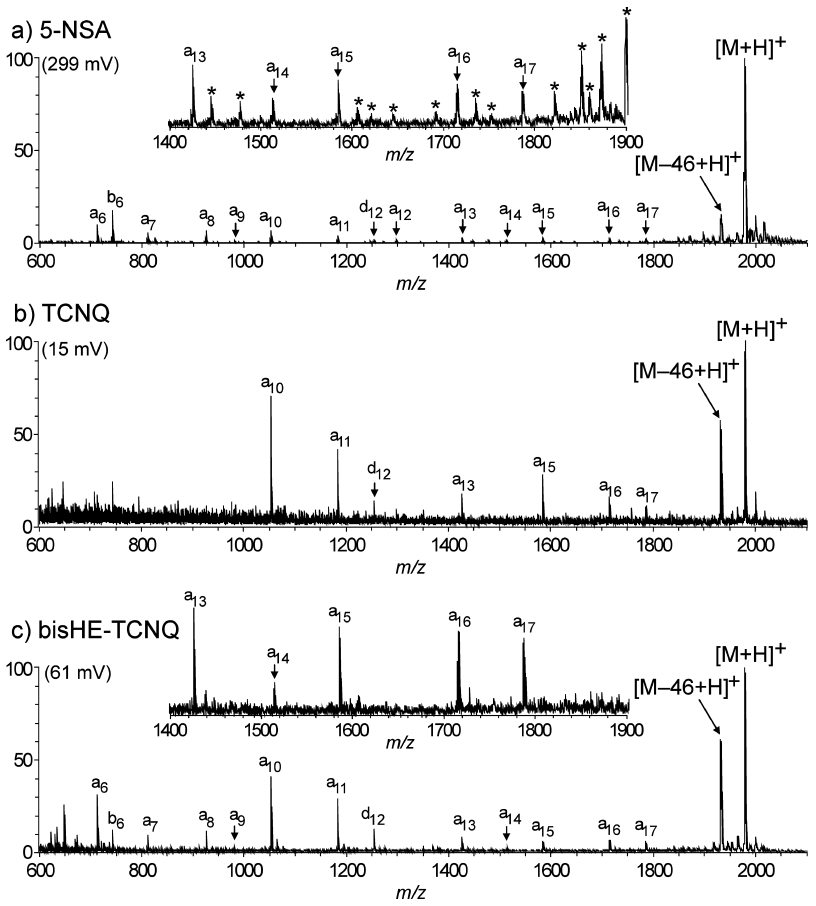

Figure 1. Positive-ion MALDI-ISD spectra of ACTH18-35 obtained with (a) 5-NSA, (b) TCNQ, and (c) bisHE-TCNQ. The insets represent the partial mass spectra in the range of m/z 1400−1900. Asterisks indicate metastable peaks.

a' and x' fragments are 1.0078 Da larger than $a\bullet$ and $x\bullet$ fragments. Unless noted otherwise, all assigned peaks represent singly protonated molecules.

RESULTS AND DISCUSSION

Matrix Effect on the In-Source Decay Fragmentation via Hydrogen Abstraction. Figure 1 shows the comparison of MALDI-ISD spectra of ACTH18-35 obtained with three different matrixes 5-NSA, TCNQ, and bisHE-TCNQ. In the MALDI-ISD with 5-NSA, the C_α−C bonds are preferentially cleaved, leading to the formation of a-series ions via the abstraction of a hydrogen atom from the peptide backbone to the matrix (Figure 1a). It has previously been reported that the TCNQ has an oxidizing nature. Although the use of TCNQ resulted in a-series ions (Figure 1b), TCNQ was a poor matrix in both normal MALDI and MALDI-ISD measurements. It is suggested that the proton transfer reaction from TCNQ to peptides is difficult, because TCNQ does not contain polar hydrogen atoms. To enhance the ion yield of both $[M+H]^+$ and ISD fragment ions, bisHE-TCNQ was used. The difference between the TCNQ and bisHE-TCNQ is the alteration of hydroxyethoxy groups at the 2- and 5-positions. Comparison of parts b and c of Figure 1 indicates that the presence of hydroxyl groups in the bisHE-TCNQ contributes to the increase in the ion yields of both $[M+H]^+$ and ISD fragment ions. Although the hydroxyl group has not only a proton-donating nature but also a hydrogen-radical-donating property, it has been suggested that the 5-hydroxyl group in 2,5-DHB plays a role in the hydrogen transfer from matrix to analyte peptide, leading to c' and z'-series fragments.[16] This can be explained by the extraordinary stability of phenoxy radical.[26] However, a functional role of bisHE-TCNQ which leads to a- and x-series ion formation originates from the hydrogen-accepting nature of CN groups. Taking this into account, it is reasonable to presume that the hydroxyl groups of bisHE-TCNQ mainly generate protons to increase the yields of protonated species, while hydrogen radicals from bisHE-TCNQ may be captured by the counterpart bisHE-TCNQ.

The MALDI-ISD with bisHE-TCNQ shows the higher S/N ratio of ISD fragment ions compared with the use of 5-NSA. Furthermore, the use of bisHE-TCNQ resulted in fewer metastable signals than that observed in the MALDI-ISD with 5-NSA, as shown in the inset of Figure 1. The high degree of metastable decay originates from the contents of internal energy in the vibrationally excited molecules. Fewer metastable signals with the use of bisHE-TCNQ indicate that the chemical bisHE-TCNQ can be classified as a more "cool" matrix than 5-NSA. The outstanding characteristics of the MALDI-ISD spectrum obtained with bisHE-TCNQ compared with 5-NSA were the high quality separation of isotope peaks of the $[M+H]^+$ and ISD ions, as shown in Figure 2. The peak broadening originates from the initial velocity dispersion of analyte ions. The sharpness in the ion peaks in the MALDI-ISD spectra with bisHE-TCNQ was maintained even at higher laser fluencies which are suitable for the appearance of ISD ion peaks. Therefore, using bisHE-TCNQ, the ISD ions could be clearly assigned due to the decreased interference peak and the sharpness of the ISD ion peaks in the MALDI-ISD spectrum.

dx.doi.org/10.1021/jp210728s | J. Phys. Chem. B 2012, 116, 4016−4023

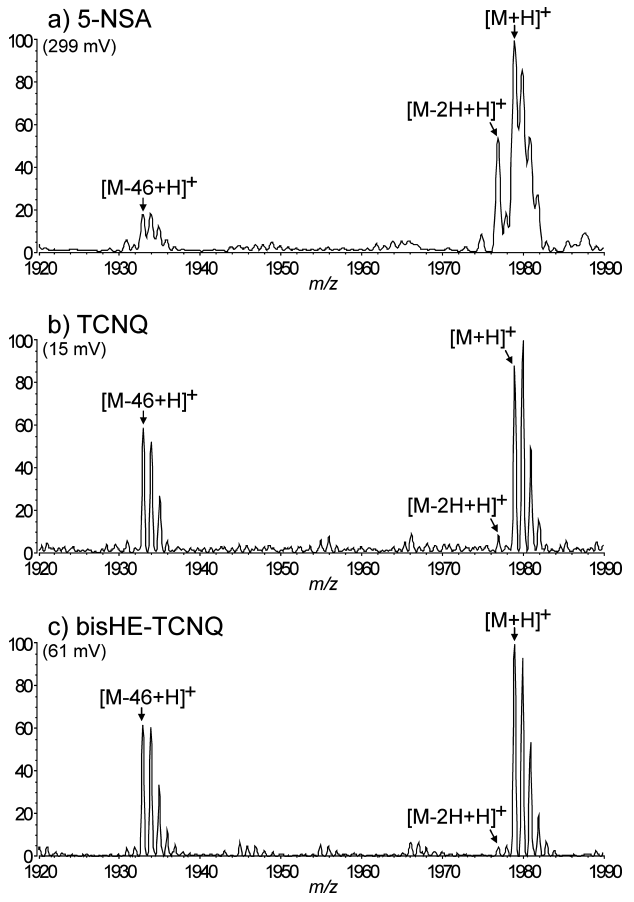

Figure 2. Partial MALDI mass spectra of ACTH18-35 obtained with (a) 5-NSA, (b) TCNQ, and (c) bisHE-TCNQ.

It was previously reported that the use of oxidizing matrixes generated the *a*- and *x*-series ions accompanied the oxidized product $[M-2H+H]^+$, as shown in Figure 2.[18] Hydrogen abstraction from peptide results in the formation of a hydrogen-deficient peptide radical $[M-H]\bullet$ where the radical site is on the amide nitrogen. Subsequently, further hydrogen abstraction from peptide radical to matrix leads to the formation of $[M-2H+H]^+$, as shown in Scheme 4. The formation of $a\bullet/x$-series

Scheme 4. Hydrogen Abstraction from Hydrogen-Deficient Peptide Radical

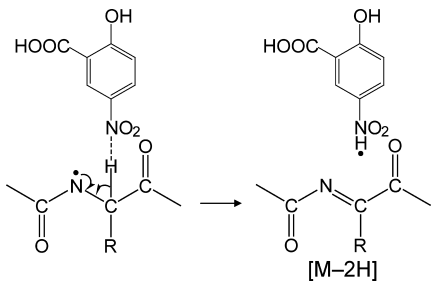

ions and $[M-2H+H]^+$ from hydrogen-deficient peptide radicals therefore competitively occurs during MALDI-ISD via hydrogen abstraction. As shown in Figure 2, 5-NSA highly favor the formation of $[M-2H+H]^+$ compared with TCNQ and bisHE-TCNQ. The same trend was obtained with other peptides, namely, [Sar[9], Met$(O_2)^{11}$]-substance P and bradykinin potentiator B. The ratio of the signal intensity of oxidized ion $[M+H-2H]^+$ to that of the nonoxidized ion $[M+H]^+$ of peptides is summarized in Table 2.

Table 2. The Ratio of Signal Intensity of Oxidized Ion $[M+H-2H]^+$ to That of Non-Oxidized Ion $[M+H]^+$ of Peptides (%)

	bisHE-TCNQ	TCNQ	5-NSA
ACTH18-35	7.0 ± 2.6	9.8 ± 2.7	51.5 ± 7.3
[Sar[9], Met$(O_2)^{11}$]-substance P	8.3 ± 1.1	15.0 ± 3.4	48.8 ± 7.0
bradykinin potentiator B	9.1 ± 1.7	13.2 ± 1.5	45.2 ± 4.2

Relationship between Initial Velocity of Ions and ISD Fragmentation. As described above, the use of 5-NSA highly favors the further hydrogen abstraction from hydrogen-deficient peptide radicals compared with TCNQ and bisHE-TCNQ. We focus on the formation mechanism of $[M-2H]$ in MALDI-ISD via hydrogen abstraction. It has been reported that the ISD fragmentation process could depend on the delay time and the ISD fragmentation occurs rapidly after desorption/ionization.[27,28] When oxidizing matrix was used, the intensity of ISD fragment ions also depended on the delay time. This suggests that the MALDI-ISD processes, at least fragmentation of peptide radicals, occur in the MALDI plume. However, the hydrogen detachment from the hydrogen-deficient peptide radical is less likely to occur in the MALDI plume. The hydrogen abstraction reactions from the hydrogen-deficient peptide radical must occur by the collision between hydrogen-deficient peptide radicals and matrix molecules in the MALDI plume (Scheme 4). Therefore, it is suggested that the ion yield of oxidized peptide $[M+H-2H]^+$ depends on the collision rate of analyte molecules in the MALDI plume. Spengler and Kirsch proposed a desorption model in MALDI.[29] According to this model, analyte molecules/ions are desorbed from matrix crystal and accelerated by collisions with matrix molecules/ions. Therefore, the high collision rate leads to a fast acceleration process, giving a high velocity of analyte molecules/ions. The velocity before the ion extraction is called "initial velocity". It has been previously reported that the initial velocity of analyte ions is dependent on the matrix.[30,31] The use of 5-NSA would be expected to give a higher initial velocity of analyte ions compared to the use of TCNQ and bisHE-TCNQ in the MALDI experiment.

The axial initial velocity of analyte ions could be measured using a linear TOF mass spectrometer. We compared the slope for time-of-flight versus delay time for the three different oxidizing matrixes 5-NSA, TCNQ, and bisHE-TCNQ. Figure 3 shows the influence of the nature of the matrix on the slope of that in the MALDI-ISD conditions for the protonated ACTH18-35. The slope of that is the proportional axial initial velocity of analyte ions.[30,31] We also acquired the slope of the TOF curve versus delay time for CHCA and 2,5-DHB as a control. The ratio of the axial initial velocity of CHCA to that of the 2,5-DHB was 1.81, and it was in good agreement with previous reports.[31] When the axial initial velocity of analyte ions was normalized to 1 for bisHE-TCNQ, slope values associated with other oxidizing matrixes were 1.21 for TCNQ and 3.04 for 5-NSA. Similar trends were observed for [Sar[9], Met$(O_2)^{11}$]-substance P and bradykinin potentiator B (data not shown). The use of 5-NSA produces analyte ions with higher initial velocity compared with TCNQ derivatives and thus increases the collision rate between the analyte and matrix molecules.

dx.doi.org/10.1021/jp210728s | J. Phys. Chem. B 2012, 116, 4016−4023

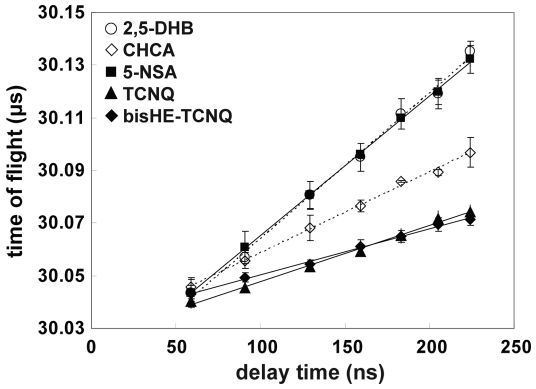

Figure 3. Representation of the variation of the time-of-flight of protonated ACTH18-35 with the delay time for the five different matrixes: 2,5-DHB, CHCA, 5-NSA, TCNQ, and bisHE-TCNQ.

When the 5-NSA was used, the high ion yield of $[M+H-2H]^+$ could be attributed to the high collision rate in the MALDI plume.

Next, we focus on the $C_\alpha-C$ bond cleavages in MALDI-ISD via hydrogen abstraction. It was previously reported that the $C_\alpha-C$ bond cleavages also occur in the negative-ion electrospray based fragmentation techniques, such as electron detachment dissociation (EDD)[32] and negative electron transfer dissociation (NETD).[33] MALDI-ISD with oxidizing matrix shares some similarities with EDD and NETD. Both EDD and NETD involve detaching electrons from multiply deprotonated analytes $[M-nH]^{n-}$ to form a charge reduced peptide anion $[M-nH]^{(n-1)-}\bullet$ that contains a radical site on the carboxyl group of the side chain or C-terminal carboxyl group. Subsequently, a nitrogen-centered radical product is formed via hydrogen transfer from the backbone amide nitrogen to the radical site on the carboxyl group. The radical site on the amide nitrogen induces dissociation of the $C_\alpha-C$ bond. In the EDD and NECD, the $C_\alpha-C$ bond cleavages occur by a unimolecular dissociation process. Additionally, an *ab initio* calculation showed that the $C_\alpha-C$ bond cleavage to produce the $a\bullet/x$ fragment pair is nearly thermo-neutral.[34] The results obtained here suggest that the $C_\alpha-C$ bond cleavages of the hydrogen-deficient peptide radical occur by a unimolecular dissociation process and independently of the collision rate in the MALDI plume. The cleavage at the $C_\alpha-C$ bond and further hydrogen atom loss of the hydrogen-deficient peptide radical competitively occur during MALDI-ISD processes. When the TCNQ derivative matrix is used, the low abundance of $[M-2H+H]^+$ and high abundance of *a*-series ions compared with 5-NSA can be understood as resulting from the low collision rate in the MALDI plume. The same trend was obtained with other peptides, namely, $[Sar^9, Met(O_2)^{11}]$-substance P, as shown in Figure 4.

Hydrocarboxyl Radical Loss from Oxidized Peptide Radical. The fragment ions $[M-46+H]^+$ were clearly observed in the MALDI-ISD spectra of ACTH18-35 (Figure 2). The fragment ions $[M-46+H]^+$ might be assigned as the loss of HCOOH from the C-terminal carboxyl group. In contrast, $[M-46+H]^+$ is not observed in MALDI-ISD with 2,5-DHB and 5-ASA and instead the fragment ion $[M-44+H]^+$ is detected.[35] The data suggests that the use of oxidizing matrixes leading to the formation of $[M-46+H]^+$ accompanies hydrogen abstraction. Hydrogen abstraction from the peptide results in the formation of the hydrogen-deficient peptide radical. Subsequently, the radical induces dissociation of the $C_\alpha-C$ bond, leading to the formation of $[M-46+H]^+$ and hydrocarboxyl radical (•COOH), as shown in Scheme 5. The signal intensity

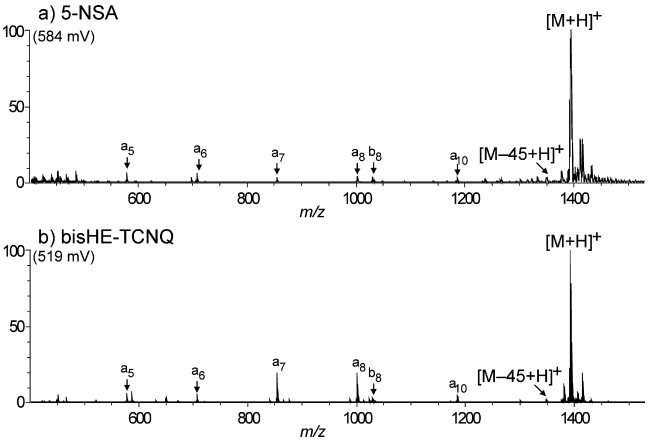

Figure 4. Positive-ion MALDI-ISD spectra of $[Sar^9, Met(O_2)^{11}]$-substance P obtained with (a) 5-NSA and (b) bisHE-TCNQ.

Scheme 5. Formation Mechanism of the [M−46]

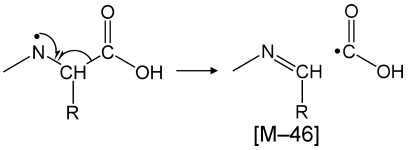

of $[M-46+H]^+$ in MALDI-ISD with TCNQ and bisHE-TCNQ was higher than that in MALDI-ISD with 5-NSA (Figure 2). The formation of [M−46] and [M−2H] from hydrogen-deficient peptide radical occurs competitively, and bisHE-TCNQ highly favors the formation of [M−46] compared with 5-NSA.

In the MALDI-ISD with oxidizing matrixes, the specific cleavage of $C_\alpha-C$ bond cleavage was observed. However, the a_{12} ion corresponding to the cleavage at the Asp−Glu bond was not observed and instead the d_{12} ion was detected in the MALDI-ISD spectrum of ACTH18-35 with bisHE-TCNQ (Figure 1c). Figure 5 shows the comparison of partial MALDI-ISD spectra of ACTH18-35 obtained with 5-NSA and bisHE-TCNQ. The d_{12} ion was also observed in the MALDI-ISD with 5-NSA. This suggests that the $a_{12}\bullet$ radical fragment further degrades to give the d_{12} fragment and •COOH radical, as shown in Scheme 6. The formation of the d_{12} fragment is due to a similar mechanism to that of the [M−46]. The loss of the hydrogen radical and •COOH radical from $a_{12}\bullet$ competitively occurs during MALDI-ISD via hydrogen abstraction (Scheme 6), and bisHE-TCNQ highly favors the •COOH radical loss compared with 5-NSA. Those data suggest that the •COOH radical loss from $[M-H]\bullet$ and $a_{12}\bullet$ radicals occurs via a unimolecular dissociation process. The high ion yield of $[M-46+H]^+$ and d_{12} might be attributed to the low collision rate in the plume using bisHE-TCNQ as a matrix.

Formyl Radical Loss from b•-Series Radical Fragments. The specific cleavage of CO−N bond cleavage at Xxx−Pro was observed *via* hydrogen abstraction from the $C_\alpha-H$ in the Pro residue.[19] The CO−N bond cleavage leads to the formation of the $b\bullet/y$ fragment pair (Scheme 2). The *a*- and *b*-series ions are generated by the formyl radical (•CHO) and hydrogen radical loss from the $b\bullet$ radical fragment, respectively

dx.doi.org/10.1021/jp210728s | J. Phys. Chem. B 2012, 116, 4016−4023

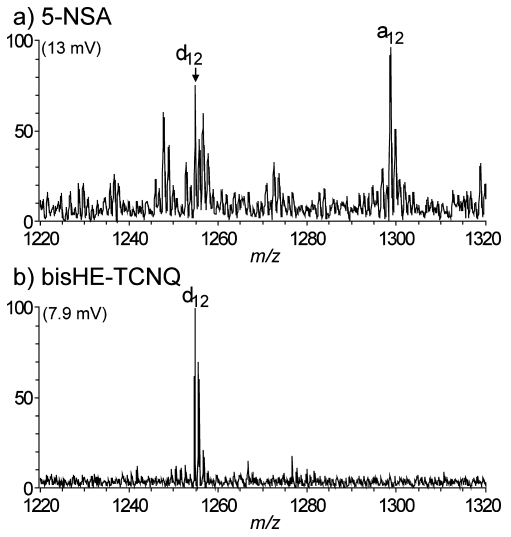

Figure 5. Partial MALDI mass spectra of ACTH18-35 obtained with (a) 5-NSA and (b) bisHE-TCNQ.

Scheme 6. The Formation Mechanisms of (a) d_{12} and (b) a_{12} Fragments from a_{12}• Radical Fragment

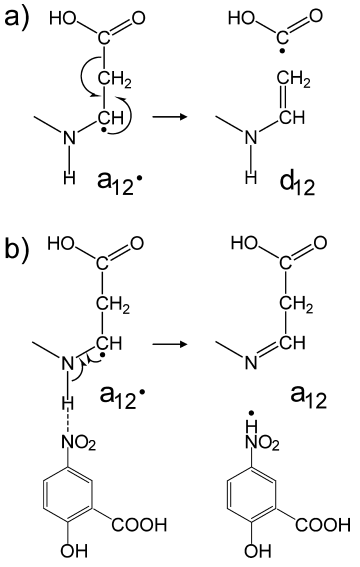

(Scheme 7). The formation of *a*- and *b*-series ions from *b*•-series ions competitively occurs during MALDI-ISD via hydrogen abstraction. To obtain the information of the mechanism for *a*- and *b*-series ion formation originated from the cleavage of the CO−N bond at the Pro residue, Pro-rich sequence peptide bradykinin potentiator B (Pyr-GLPPRPKIPP) was used for MALDI-ISD experiment. Figure 6 shows the comparison of MALDI-ISD spectra of bradykinin potentiator B obtained with 5-NSA and bisHE-TCNQ. The use of those matrixes generated the *a*- and *b*-series ions originated from the cleavage at Xxx−Pro bonds. The *b*-series ions generated from bisHE-TCNQ were generally less intense than those generated from 5-NSA. Therefore, the use of bisHE-TCNQ highly favors the loss of formyl radical from the *b*• radical fragment compared with 5-NSA (Scheme 7). The same trend was obtained with other peptides, namely, ACTH18-35 and [Sar^9, Met(O$_2$)^{11}]-substance P, as shown in Figures 1 and 4, respectively. The cleavage of CO−N bonds was observed at the Tyr^6−Pro^7 bond in ACTH18-35 and the Phe^8−Sar^9 bond

Scheme 7. The Formation Mechanisms of (a) *a*- and (b) *b*-Series Fragments from the *b*•-Series Radical Fragment

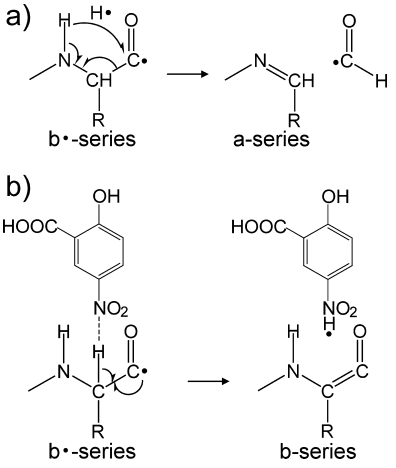

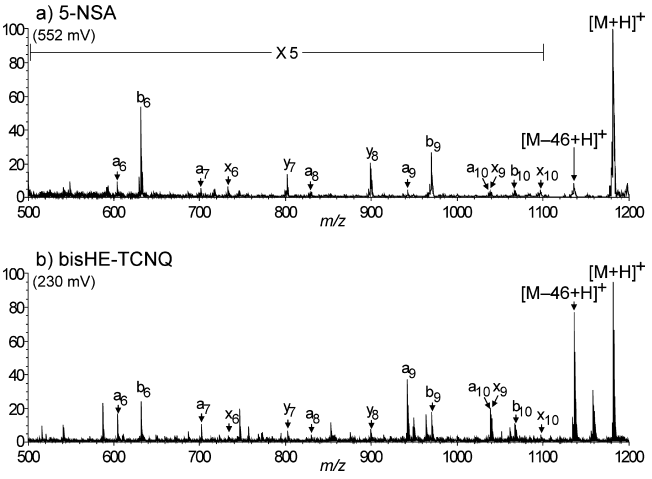

Figure 6. Positive-ion MALDI-ISD spectra of bradykinin potentiator B obtained with (a) 5-NSA and (b) bisHE-TCNQ.

in [Sar^9, Met(O$_2$)^{11}]-substance P. In both cases, the use of bisHE-TCNQ gave the higher intensity of *a*-series ions compared with the use of 5-NSA. This suggests that the formation of *a*-series fragments from *b*•-series radical fragments occurs via a unimolecular dissociation process. The high ion yield of *a*-series ions and low ion yield of *b*-series ions might be attributed to the low collision rate in the plume using bisHE-TCNQ as a matrix.

■ CONCLUSION

The MALDI-ISD of peptides has been studied using 5-NSA, TCNQ, and bisHE-TCNQ as matrixes. The fragmentation processes *via* hydrogen-deficient peptide [M−H]• containing a radical site on the amide nitrogen are summarized in Scheme 8. The hydrogen-deficient peptide gave the *a*•/*x* fragment pair and [M−2H]. The preferential formation of [M+H−2H]$^+$ was found to be dependent on the initial velocity of analytes, which is proportional to the collision rate of analytes in the MALDI plume. Therefore, it is suggested that the further hydrogen abstraction from [M−H]• to form [M−2H] is induced by collisions between hydrogen-deficient peptide radicals and matrix molecules in the MALDI plume. In contrast, the C_α−C bond cleavages occur via a unimolecular dissociation process and independently of the collision rate in the MALDI plume.

dx.doi.org/10.1021/jp210728s | J. Phys. Chem. B 2012, 116, 4016−4023

Scheme 8. Fragmentation Processes via Hydrogen-Deficient Peptide [M−H]• Containing a Radical Site on the Amide Nitrogen[a]

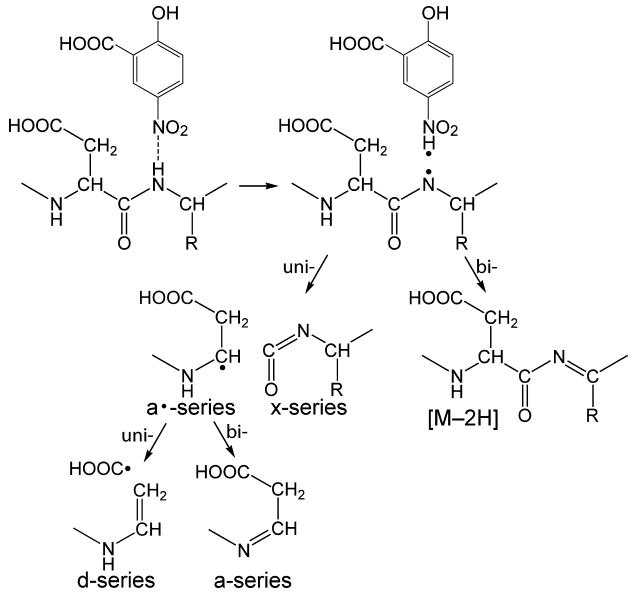

[a]"uni-" and "bi-" denote uni-molecular decay process and bi-molecular reaction, respectively.

The radical fragments *a*•-series ions are not observed, whereas the *a*•/*x* fragment pairs were formed by the C_α−C bond cleavage. It is likely that there are sufficient amounts of matrix molecules in the MALDI plume to form the *a*-series ions via the further hydrogen abstraction after the C_α−C bond cleavage. The *a*• radical fragment originated from the cleavage at Asp−Xxx gives not only an *a*-series fragment, but also a *d*-series fragment by the •COOH radical loss. The further hydrogen abstraction from *a*•-series radicals to form *a*-series fragments was also dependent on the collision rate in the MALDI plume. In contrast, the •COOH radical loss occurs via the unimolecular dissociation process.

The fragmentation processes of the Xxx−Pro bond *via* hydrogen abstraction are summarized in Scheme 9. The cleavage at the CO−N bond of Xxx−Pro occurs with hydrogen abstraction from C_α−H in the Pro residue, leading to the formation of the *b*•/*y*-series fragment pair. The loss of hydrogen radical and •CHO radical from *b*•-series radical gives *b*- and *a*-series fragments, respectively. The hydrogen abstraction from *b*•-series radical to form *b*-series fragment was also dependent on the collision rate in the MALDI plume, and the •CHO radical loss of *b*•-series radical occurs via a unimolecular dissociation process.

In the MALDI-ISD with oxidizing matrix, the hydrogen abstraction and decay process from analyte radicals occur competitively. It was concluded that the further hydrogen abstraction from analyte radicals such as [M−H]•, *a*•- and *b*•-series induced by collision with matrix molecules in the MALDI plume. In contrast, decay processes such as the C_α−C and CO−N bond cleavages of [M−H]• and further degradation of radical products occur via unimolecular dissociation. When the bisHE-TCNQ derivative matrix is used, the low abundance of $[M-2H+H]^+$ and high abundance of *a*-series ions compared with 5-NSA can be understood as resulting from the low collision rate in the MALDI plume.

Scheme 9. The Fragmentation Processes of Xxx−Pro Bond via Hydrogen Abstraction[a]

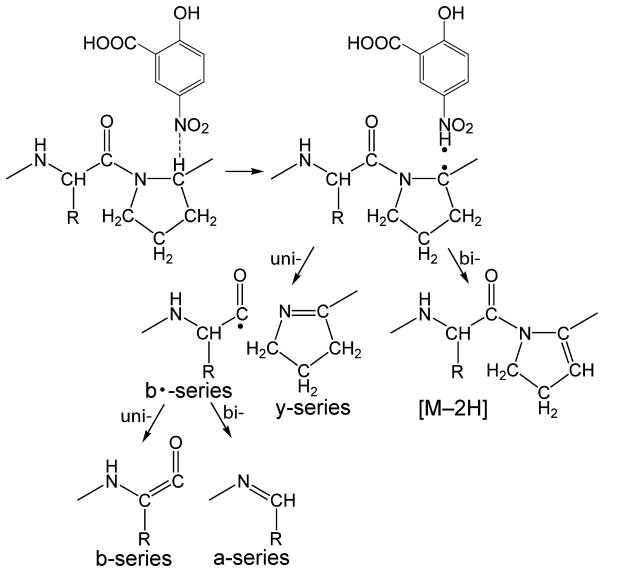

[a]"uni-" and "bi-" denote uni-molecular decay process and bi-molecular reaction, respectively.

AUTHOR INFORMATION

Corresponding Author

*E-mail: takayama@yokohama-cu.ac.jp.

Notes

The authors declare no competing financial interest.

ACKNOWLEDGMENTS

D.A. acknowledges the research fellowship from the Japan Society for the Promotion of Science for Young Scientists (23-10272). M.T. acknowledges support from the Creation of Innovation Centers for Advanced Interdisciplinary Research Area in the Special Coordination Fund for Promoting Science and Technology, and a Grant-in-Aid for Scientific Research (C) (23550101) from the Japan Ministry of Education, Culture, Sports, and Technology.

REFERENCES

(1) Karas, M.; Bachmann, D.; Bahr, U.; Hillenkamp, F. *Int. J. Mass Spectrom. Ion Processes* **1987**, *78*, 53−68.

(2) Tanaka, K.; Waki, H.; Ido, Y.; Akita, S.; Yoshida, Y.; Yoshida, T. *Rapid Commun. Mass Spectrom.* **1988**, *2*, 151−153.

(3) Karas, M.; Hillenkamp, F. *Anal. Chem.* **1988**, *60*, 2299−2301.

(4) Whitehouse, C. M.; Dreyer, R. N.; Yamashita, M.; Fenn, J. B. *Anal. Chem.* **1985**, *57*, 675−679.

(5) Fenn, J. B.; Mann, M.; Meng, C. K.; Wong, S. F.; Whitehouse, C. M. *Science* **1989**, *246*, 60−71.

(6) Henzel, W. J.; Billeci, T. M.; Stults, J. T.; Wong, S. C.; Grimley, C.; Watanabe, C. *Proc. Natl. Acad. Sci. U.S.A.* **1993**, *90*, 5011−5015.

(7) Pappin, D. J. C.; Hojrupt, P.; Bleasbyl, A. J. *Curr. Biol.* **1993**, *3*, 327−332.

(8) Brown, R. S.; Lennon, J. J. *Anal. Chem.* **1995**, *67*, 3990−3999.

(9) Spengler, B.; Kirsch, D.; Kaufmann, R.; Jaeger, E. *Rapid Commun. Mass Spectrom.* **1992**, *6*, 105−108.

(10) Kaufmann, R.; Spengler, B.; Lützenkirchen, F. *Rapid Commun. Mass Spectrom.* **1993**, *7*, 902−910.

(11) Hardouin, J. *Mass Spectrom. Rev.* **2007**, *26*, 672−682.

(12) Chaurand, P.; Luetzenkirchen, F.; Spengler, B. *J. Am. Soc. Mass Spectrom.* **1999**, *10*, 91−103.

(13) Reiber, D. C.; Grover, T. A.; Brown, R. S. *Anal. Chem.* **1998**, *70*, 673−683.
(14) Takayama, M. *J. Mass Spectrom. Soc. Jpn.* **2002**, *50*, 304−310.
(15) Suckau, D.; Resemann, A. *Anal. Chem.* **2003**, *75*, 5817−5824.
(16) Takayama, M. *J. Am. Soc. Mass Spectrom.* **2001**, *12*, 1044−1049.
(17) Köcher, T.; Engström, A.; Zubarev, R. A. *Anal. Chem.* **2005**, *77*, 172−177.
(18) Asakawa, D.; Takayama, M. *J. Am. Soc. Mass Spectrom.* **2011**, *22*, 1224−1233.
(19) Asakawa, D.; Takayama, M. *Rapid Commun. Mass Spectrom.* **2011**, *25*, 2379−2383.
(20) Asakawa, D.; Takayama, M. *J. Mass Spectrom.* **2012**, *47*, 180−187.
(21) Przybilla, L.; Brand, J.-D.; Yoshimura, K.; Räder, H. J.; Müllen, K. *Anal. Chem.* **2000**, *72*, 4591−4597.
(22) Trimpin, S.; Rouhanipour, A.; Az, R.; Räder, H. J.; Müllen, K. *Rapid Commun. Mass Spectrom.* **2001**, *15*, 1364−1373.
(23) Trimpin, S.; Grimsdale, A. C.; Räder, H. J.; Müllen, K. *Anal. Chem.* **2002**, *74*, 3777−3782.
(24) Asakawa, D.; Chen, L. C.; Hiraoka, K. *J. Mass Spectrom.* **2008**, *43*, 1494−1501.
(25) Zubarev, R. A. *Mass Spectrom. Rev.* **2003**, *22*, 55−77.
(26) de Heer, M. I.; Mulder, P.; Korth, H.-G.; Ingold, K. U.; Lusztyk, J. *J. Am. Chem. Soc.* **2000**, *122*, 2355−2360.
(27) Brown, R. S.; Carr, B. L.; Lennon, J. J. *J. Am. Soc. Mass Spectrom.* **1996**, *7*, 225−232.
(28) Takayama, M. *J. Am. Soc. Mass Spectrom.* **2001**, *12*, 420−427.
(29) Spengler, B.; Kirsch, D. *Int. J. Mass Spectrom.* **2003**, *226*, 71−83.
(30) Juhasz, P.; Vestal, M. L.; Martin, S. A. *J. Am. Soc. Mass Spectrom.* **1997**, *8*, 209−217.
(31) Glückmann, M.; Karas, M. *J. Mass Spectrom.* **1999**, *34*, 467−477.
(32) Budnik, B. A.; Haselmann, K. F.; Zubarev, R. A. *Chem. Phys. Lett.* **2001**, *342*, 299−302.
(33) Coon, J. J.; Shabanowitz, J.; Hunt, D. F.; Syka, J. E. P. *J. Am. Soc. Mass Spectrom.* **2005**, *16*, 880−882.
(34) Anusiewicz, I.; Jasionowski, M.; Skurski, P.; Simons, J. *J. Phys. Chem. A* **2005**, *109*, 11332−11337.
(35) Sakakura, M.; Takayama, M. *J. Am. Soc. Mass Spectrom.* **2010**, *21*, 979−988.